Microtubule flux in mitosis is independent of chromosomes, centrosomes, and antiparallel microtubules

Molecular Biology of the Cell
Vol. 5, 217–226, February 1994

Microtubule Flux in Mitosis Is Independent of Chromosomes, Centrosomes, and Antiparallel Microtubules

Kenneth E. Sawin* and Timothy J. Mitchison†

Departments of *Biochemistry and Biophysics and †Pharmacology, University of California, San Francisco, California 94143-0448

Submitted November 12, 1993; Accepted December 23, 1993
Monitoring Editor: James A. Spudich

We investigated the mechanism of poleward microtubule flux in the mitotic spindle by generating spindle subassemblies in *Xenopus* egg extracts in vitro and assaying their ability to flux by photoactivation of fluorescence and low-light multichannel fluorescence videomicroscopy. We find that monopolar intermediates of in vitro spindle assembly (half-spindles) exhibit normal poleward flux, as do astral microtubule arrays induced by the addition of dimethyl sulfoxide to egg extracts in the absence of both chromosomes and conventional centrosomes. Immunodepletion of the kinesin-related microtubule motor protein Eg5, a candidate flux motor, suggests that Eg5 is not required for flux. These results suggest that poleward flux is a basic element of microtubule behavior exhibited by even simple self-organized microtubule arrays and presumably underlies the most elementary levels of spindle morphogenesis.

INTRODUCTION

The mitotic spindle, a complex bipolar array of microtubules and associated proteins and subcellular structures, provides the structural framework for the accurate partitioning of chromosomes in mitosis (Mazia, 1961; Nicklas, 1971; Inoue, 1981; McIntosh and Koonce, 1989; Karsenti, 1991). The spindle is constructed rapidly from preexisting components at the onset of mitosis and subsequently disassembled at its close. Understanding the structure and dynamics of the spindle is critical to a more complete understanding of mitotic mechanisms. The pioneering experiments of Inoue and collaborators (Inoue and Sato, 1967; Inoue and Ritter, 1975), which proved the existence of microtubules (spindle fibers) in vivo, also showed that spindle microtubules are highly dynamic. Most microtubule turnover is characterized by a process termed dynamic instability, in which microtubules transit stochastically between growing and shrinking phases (Mitchison and Kirschner, 1984), with characteristic transition frequencies between the two states (Walker *et al.*, 1988). Rates of microtubule turnover are increased in mitosis versus interphase, regulated by the activity of the cdc2-cyclin kinase (Belmont *et al.*, 1990; Verde *et al.*, 1990), and this is reflected in the short half-lives characteristic of most spindle microtubules (Salmon *et al.*, 1984; Saxton *et al.*, 1984).

In addition to dynamic instability, spindle microtubules can exhibit a second kind of dynamics. Marking experiments using a photoactivatable fluorescent tubulin analogue have shown that microtubules can turn over vectorially, through the disassembly of microtubules at their "minus" ends (near spindle poles), countered by the continuous assembly of new tubulin subunits at "plus" ends (Mitchison, 1989). These concerted assembly/disassembly reactions are coupled to the wholesale movement of the microtubule lattice, such that a photoactivated mark made on spindle microtubules at an early time will have moved closer toward the proximal spindle pole at a later time. This phenomenon has been termed poleward microtubule flux. Poleward flux is observed both in tissue culture cell lines (Mitchison, 1989) and in primary cultures (Mitchison and Salmon, 1992), as well as in spindles assembled in *Xenopus* egg extracts in vitro (Sawin and Mitchison, 1991b). Studies of poleward flux in vitro suggest that the two behaviors of dynamic instability and poleward flux are superimposable; this combination of these behaviors is summarized in Figure 1. Interestingly, microtubules from opposite spindle poles are able to flux or slide against each other

in spindles in vitro, in spite of maintenance of spindle shape and size. Thus, the apparent steady-state metaphase spindle is in a complex state of "dynamic order," in which global morphology remains for the most part unchanged against a background of dynamic instability and poleward flux.

Neither the molecular mechanisms governing microtubule flux nor its function in mitosis is understood. With regard to mechanism, we would like to know the following: 1) what elements of spindle architecture are involved in poleward flux? 2) what is the nature of force generation for poleward movement of microtubules, i.e., what is the "motor" for flux? and 3) where does this motor reside? The geometry of poleward microtubule flux, in which the microtubule lattice moves with minus-ends leading, and the complete inhibition of flux by the kinesin inhibitor AMP-PNP (Sawin and Mitchison, 1991b) have suggested that flux could be driven by a plus-end directed microtubule motor protein, perhaps a kinesin-like protein. Such a motor could be localized to any number of distinct sites in the spindle, among them antiparallel microtubules, spindle poles, chromosomes, and a hypothetical "matrix" of spindle components associated with microtubules but disperse throughout the spindle (Sawin and Mitchison, 1991b). An alternative view of mechanism might be that poleward flux does not require a distinct "motor" but rather is driven energetically by the thermodynamics of tubulin polymerization/depolymerization at microtubule ends (see Discussion, below). Understanding the structural and molecular basis of poleward flux will yield clues to its function; for example, if force-producing machinery for flux were localized to antiparallel microtubules, it could be harnessed to drive separation of spindle poles in anaphase B. By contrast, it would be difficult to envision a function for flux in pole separation if the motors themselves were localized to spindle poles.

To address these questions, we have constructed and assayed the properties of a variety of spindle-related structures in vitro, using *Xenopus* egg extracts. We find that antiparallel microtubules are not required for poleward flux. Moreover, flux persists in microtubule arrays that lack both chromosomes and centrosomes. The results suggest that poleward microtubule flux is an intrinsic property of simple microtubule arrays in mitosis. We also show that in this in vitro system, immunodepletion of Eg5, a microtubule motor protein considered a good candidate for a spindle flux motor, has no noticeable effect on poleward microtubule flux.

MATERIALS AND METHODS

Reagents

Unless otherwise specified, all chemical reagents were from Sigma (St. Louis, MO).

Fluorescent Labeling

Fluorescent tubulin labeling was performed as described previously (Sawin and Mitchison, 1991b). Phosphocellulose-purified bovine brain tubulin was labeled with X-rhodamine NHS-ester (Molecular Probes, Eugene, OR), following established methods (Hyman *et al.*, 1991). The stoichiometry of labeling was between 1.5 and 2.0 (dye molecules per tubulin dimer). Tubulin was independently labeled with C2CF-S-NHS ester (Mitchison, 1989), with the following modifications. 1) The first polymerization step before labeling was promoted with 10% dimethyl sulfoxide (DMSO) (vol/vol) rather than 33% glycerol. 2) Microtubules were labeled for 60 min at 37°C. 3) During depolymerization steps, microtubule pellets were resuspended in a minimal volume of IB (50 mM K glutamate, 0.5 mM $MgCl_2$) and sonicated carefully until the suspension was no longer turbid. In the repolymerization after cold spin, cold supernatants were supplemented with 1:5 volume 5X BRB80 (80 mM K piperazine-*N*,*N*'-bis(2-ethanesulfonic acid, 1 mM $MgCl_2$, 1 mM ethylene glycol-bis(β-aminoethyl ether)-*N*,*N*,*N*',*N*'-tetraacetic acid, pH 6.8) to favor polymerization. 4) Tubulin was cycled only once rather than twice. These modifications led to an improved yield (25% of the initial labeling reaction) and stoichiometry (0.6 dye caged-fluorescein molecules per tubulin dimer) relative to previous methods, without any apparent differences in the behavior of the labeled tubulin in our experiments.

Demembranated *Xenopus* sperm nuclei were prepared as described (Murray, 1992), except that *Xenopus* males were not primed with hormones before they were killed and 10 mM $MgCl_2$ was used in buffers in place of polyamines. Sperm were covalently labeled with CY5.18 OSu (Biological Detection Systems, Pittsburgh, PA) using a modification of our previous method (Sawin and Mitchison, 1991b). Briefly, after demembranation of sperm by lysophosphatidylcholine and quenching with bovine serum albumin (BSA), sperm were washed out of BSA and reacted with 16 μM CY5 NHS-ester for 30 s. The labeling reaction was quenched with 10 mM K glutamate. Sperm were washed and ultimately resuspended in glycerol-containing buffer (Murray, 1992) and frozen at −80°C. Single aliquots of labeled and unlabeled sperm can be freeze-thawed and stored at −80°C ≥20 times without any significant loss of activity.

Egg Extracts

Xenopus egg extracts arrested in meiotic metaphase II (i.e., "CSF extracts") were prepared as described (Murray, 1992), except that ATP-regenerating system was not used as it was found to be unnecessary.

Spindle assembly reactions were performed essentially as described (Sawin and Mitchison, 1991a,b). Labeled and/or unlabeled demembranated *Xenopus* sperm were added to extracts as a 1:10 dilution in 100 mM KCl/150 mM sucrose to a final concentration of 100 and 200 nuclei/ml extract. When appropriate, DMSO (Aldrich, St. Louis, MO, in SureSeal septum bottles) was added to extracts to 5% vol/vol final. Extracts were incubated at 20°C for 30–45 min for assembly of spindles, half-spindles, and/or DMSO asters, before mounting on microscope slides for imaging.

Antibodies

A polyclonal antibody against the Eg5 stalk was raised against a glutathione-S-transferase (GST) fusion protein containing the Eg5 stalk and tail (GST-Eg5ST). Fusion protein induced in bacteria was purified on glutathione agarose (Sawin *et al.*, 1992) and injected into New Zealand White rabbits with Freund's complete or incomplete adjuvant for primary and secondary injections, respectively. Pooled antisera were affinity-purified three times on GST coupled to Affigel 10 (Bio-Rad, Richmond, CA) to deplete antibodies to GST and were then purified against a second fusion protein containing the Eg5 head and stalk (GST-Eg5HS) coupled to Affigel to obtain stalk-specific antibodies. Antibodies were eluted with 0.2 M glycine, pH 2.0, and concentrated and dialyzed into IB before use. The anti-Eg5-stalk antibody was specific for Eg5 on immunoblots and identified a single Coomassie-stained band of the expected molecular weight after sodium dodecyl sulfate-polyacrylamide gel electrophoresis of native immunoprecipitates. Immunodepletion experiments were done as previously described (Sawin *et al.*, 1992), using 2 μg anti-stalk antibody/100 μl

CSF extract and a 20% bead volume of Affiprep protein-A (Bio-Rad). The extent of immunodepletion was quantitated by comparing the Eg5 signal on immunoblots of depleted extracts with the signal obtained in serial dilutions of mock-depleted extracts. Using this method we found that Eg5 levels in extracts could be reduced to 2–4% of normal levels on a routine basis.

Optical System and Data Collection

For these experiments we modified our original photoactivation system (Sawin and Mitchison, 1991b; Sawin *et al.*, 1993) as follows: 1) the system was built around an upright microscope (Zeiss, Thornword, NY) rather than an inverted IM35 for better light throughput; 2) a 100-μm fixed-width air slit (Melles Griot [Irvine, CA] and additional homemade components) was used for photoactivation and mounted on an optical rail attached to the microscope; and 3) our previous epifluorescence filters and dual-band dichroic mirror were replaced with a new set of custom-designed interference filters, including a novel four band-pass chromatic beam-splitter for simultaneous imaging of Hoechst or 4,6-diamidino-2-phenylindole (DAPI), fluorescein, X-rhodamine/Texas red, and CY5 (Omega Optical, Brattleboro, VT). The fluorescein, X-rhodamine, and CY5 reflections were used for imaging, whereas the Hoechst/DAPI reflection was used to steer the 360-nm photoactivation beam onto the sample. Emission filters were unblocked to increase signals, whereas excitation filters were fully blocked; the unblocked emission filters did not appear to compromise spectral separation, as we did not observe fluorescence bleedthrough, even with comparatively bright samples. The spectral characteristics of these filters are available to interested investigators. All experiments were performed with a Zeiss 100X 1.4 NA Neofluar objective. The ambient temperature with all electronics running was held to 22–23°C.

For flux assays, 6–9 μl of extracts containing spindles or related structures were spotted onto glass microscope slides and covered with 18-mm^2 coverslips, Number 1 thickness, and sealed with Valap (1:1:1 ratio of Vaseline, lanolin, and paraffin). The thickness of these chambers is calculated to be ~18 μm. Slides were then placed on the microscope, and structures suitable for photoactivation were identified by low power fluorescence and phase-contrast microscopy. Structures were aligned with respect to the known position of the photoactivation beam, using a rotating/translating stage. Photoactivation was typically 1.4–2.8 s and controlled by electronic shutter. Images were time-averaged and acquired as described (Sawin and Mitchison, 1991b; Sawin *et al.*, 1993) using an intensified silicon intensified target camera (COHU ISIT, series 5000, San Diego, CA) and Datacube (Peabody, MA) Maxvision AT image processor, running a combination of commercial and home-written software. Images were recorded onto an optical memory disc recorder (Panasonic 3031, Secaucus, NJ).

Digitized line intensity profiles were generated with Image-1 software (Universal Imaging, West Chester, PA). Analysis of data was done through a combination of manual measurements directly from the video monitor as well as automated measurements of digitized images, using Image-1. Photographs of representative images were made from the video record and printed on low contrast paper using identical exposure times and contrast; we note that the contrast reproduction of photographs is not as "true" as the digitized image data, due to the relatively low number of gray scales of the photographic paper (see, for example, Figures 4 and 6).

RESULTS

Poleward Microtubule Flux in the Half-Spindle

Bipolar spindles in CSF extracts form via the head-to-head fusion of half-spindles, monopolar microtubule arrays containing a centrosome or pole at one end and chromosomes at the other (Sawin and Mitchison, 1991a). To investigate whether bipolarity is essential

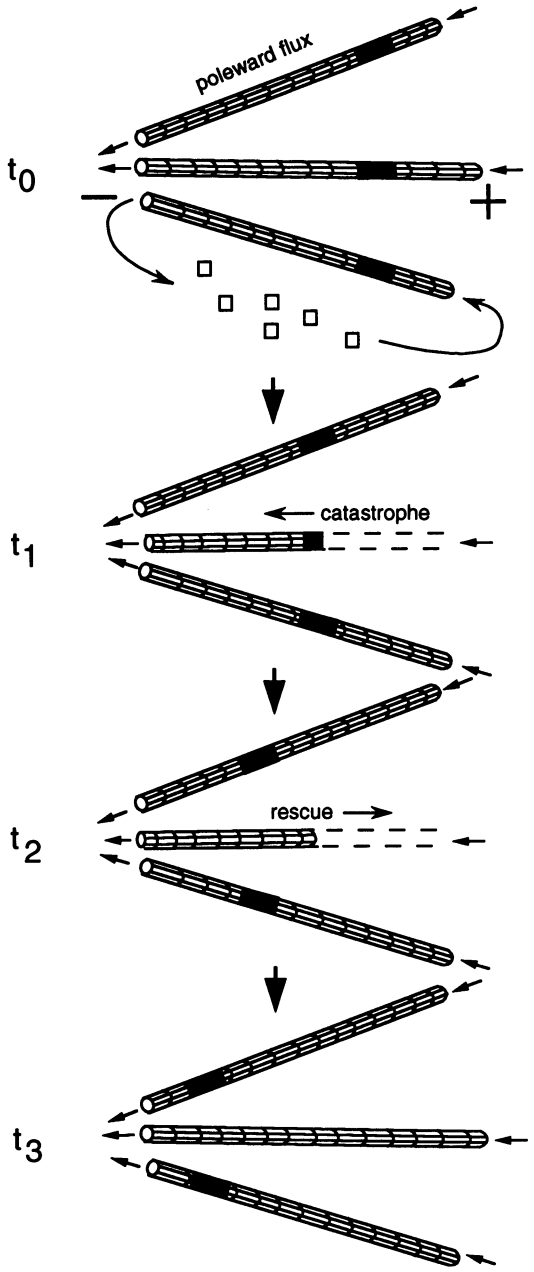

Figure 1. A schematic timecourse of lattice movements after photoactivation, illustrating simultaneous dynamic instability and poleward microtubule flux within the spindle. For simplicity, only microtubules of one polarity (from one half of the spindle) are shown, and chromosomes and centrosomes are omitted. No assumptions are made concerning the mechanism of movement. Black boxes indicate photoactivation marks on the microtubule lattice. Arrows at ends of microtubules show direction of poleward flux, with respect to microtubule ends (minus, toward the spindle pole; plus, toward the spindle equator). At t_0, treadmilling exchange of monomer and polymer pools is shown explicitly. At t_1, lattice has moved poleward, and the central microtubule has experienced a catastrophe and shrinks back (barbed arrow) past the mark, obliterating it. By t_2, the central microtubule has undergone rescue and is again elongating at its end (barbed arrow), as entire lattice continues to move poleward. By t_3, mark has moved further poleward (decreasing in total intensity), and the steady-state microtubule distribution is comparable with that seen at t_0.

for poleward flux (as would occur, for example, if flux were directly mediated by the sliding of antiparallel microtubules from opposing spindle poles), we photoactivated fluorescence in microtubules of individual half-spindles that had previously incorporated caged-fluorescein tubulin to steady state. Half-spindles also contained rhodamine-labeled tubulin and CY5-labeled chromatin as additional markers, and all three fluorochromes were followed using a computer-controlled microscope equipped for ultraviolet (UV) photoactivation and very low-light multilabel imaging (see Materials and Methods). After photoactivation via a 1-μm UV microbeam orthogonal to the half-spindle axis, we observed poleward movement of photoactivated fluorescein-tubulin in the half-spindle (Figures 2 and 3); by contrast, the position and intensity of both CY5-labeled chromosomes and rhodamine-labeled half-spindle pole remained unchanged. Poleward movement of fluorescence was linear over time and inhibited by 2 mM MgAMP-PNP, as previously demonstrated for bipolar spindles (Sawin and Mitchison, 1991b). Measurements of the rate of flux in 26 independent experiments yielded an average rate of 0.042 μm/s (SD = 0.014) (see Figure 8B), comparable with the rate of flux measured in bipolar spindles (Sawin and Mitchison, 1991b) (see Figure 8A).

Poleward Flux in Microtubule Arrays Induced by DMSO

Interactions between chromosomes and microtubules that might generate a relative poleward force on microtubules could also potentially drive poleward flux (Mitchison and Kirschner, 1985; Rieder *et al.*, 1986). In both the in vitro spindle and the half-spindle, microtubule distribution is highly biased toward chromatin (Sawin and Mitchison, 1991a), and as such it is not possible to photoactivate microtubules whose plus ends (i.e., ends away from poles) are not near chromosomes. We therefore investigated the role of chromosomes by forming microtubule arrays in the absence of sperm nuclei. In CSF extracts, the addition of microtubule-promoting agents such as taxol or DMSO induces the formation of both radially symmetric and asymmetric microtubule arrays ("taxol"- and "DMSO-asters") that lack both centrioles and conventional centrosomes, although these arrays contain morphological "poles" that accumulate at least some known centrosomal and microtubule minus-end markers, including γ-tubulin, pericentrin, and a centrosomal antigen recognized by the monoclonal antibody CTR2611 (Verde *et al.*, 1991; Stearns and Kirschner, 1994).

CSF extracts containing rhodamine- and caged-fluorescein tubulin but lacking sperm nuclei were supplemented with 5% DMSO and allowed to form asters; after photoactivation of fluorescence we observed a centripetal flux of microtubules, analogous to poleward microtubule flux (Figure 4). Digitization of fluorescence

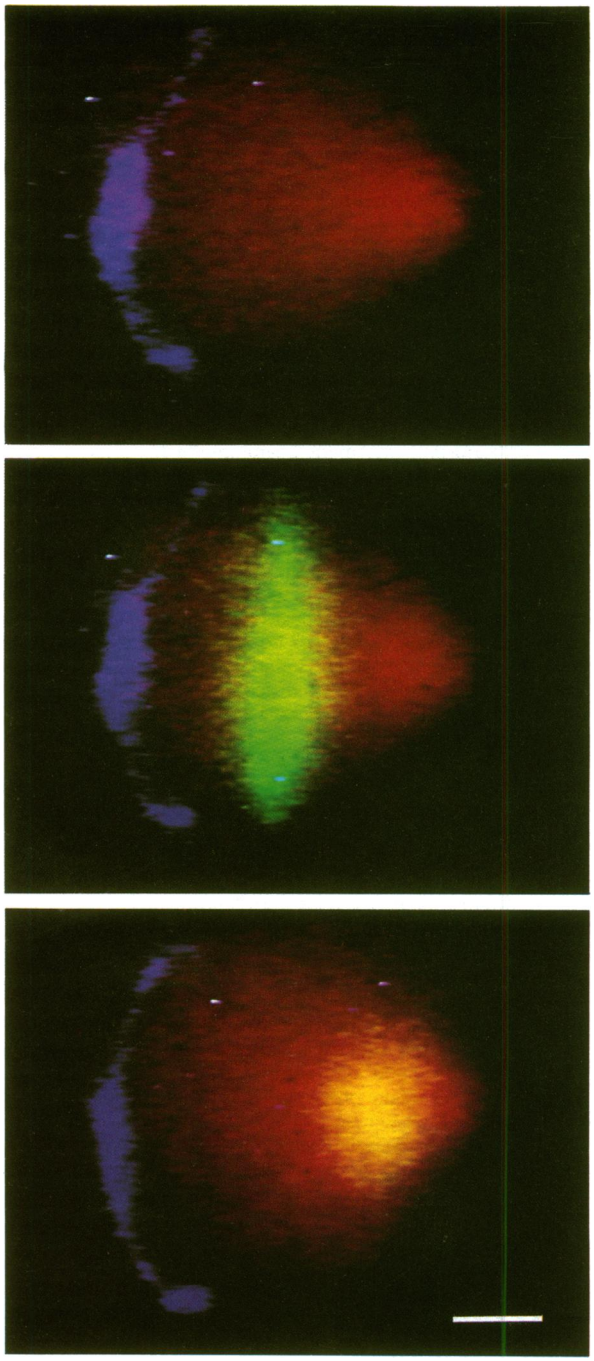

Figure 2. Poleward microtubule flux in the half-spindle. Pseudocolor images from a video sequence of a half-spindle at 12 s before and 3 and 327 s after photoactivation. Total rhodamine tubulin is shown in red, CY5-labeled chromosomes are blue, and photoactivated caged-fluorescein tubulin is green. The yellow in the final image results from the overlap of green and red at equal intensities. The decrease in fluorescein-tubulin intensity reflects microtubule turnover, whereas smaller differences in rhodamine tubulin intensity represent subtle shape changes in the half-spindle during the course of the experiment. Scale bar, 10 μm.

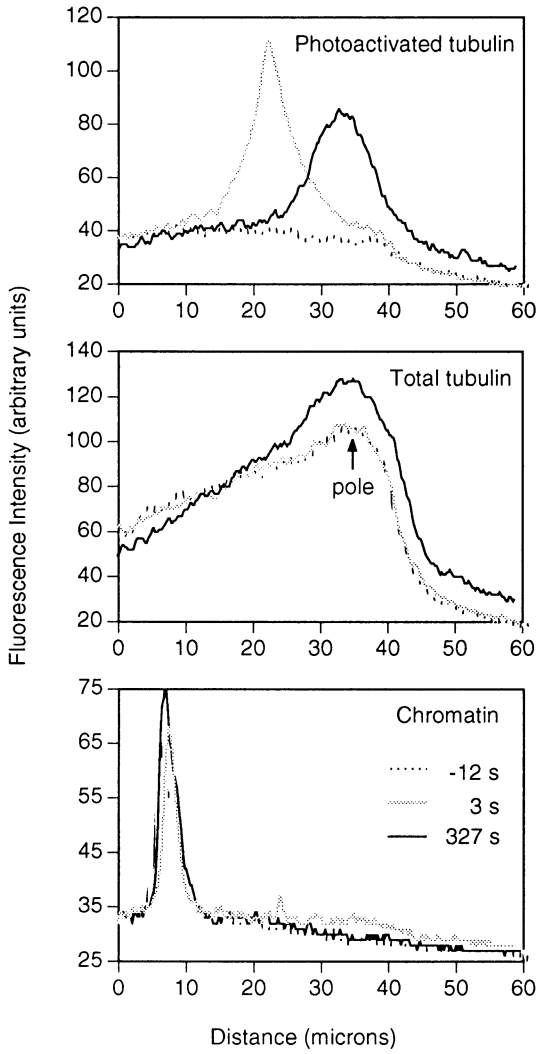

Figure 3. Digitized fluorescence intensity profiles through the half-spindle for the images shown in Figure 2. Both the "peak" and "shoulder" of photoactivated fluorescence (photoactivated tubulin) have moved rightward, whereas the position of the half-spindle pole (total tubulin) and chromatin are unchanged.

revealed that, as in half-spindles, fluorescence increased in poleward regions over time, indicating true rather than merely "apparent" poleward movement (Sawin and Mitchison, 1991b) (Figure 5). The average rate of flux in DMSO-asters in 28 independent experiments was 0.018 μm/s (SD = 0.010) (see Fig. 8C), significantly less than the rate observed in half-spindles and spindles (by Student's t test, $t = 7.47$; $p < 0.001$). Although these experiments indicate that neither chromosomes nor conventional centrosomes are required for poleward flux, because poleward flux in DMSO asters was considerably slower than in spindles and half-spindles, we investigated whether DMSO itself might exert an inhibitory effect on flux beyond its microtubule-stabilizing effects. We found that adding 5% DMSO (vol/vol) to extracts that had already formed spindles led to altered spindle morphology, characterized primarily by an increase in astral microtubules and a relative decrease of midzone microtubules, with eventual spindle dissolution. However, by marking spindles quickly after DMSO addition, we were able to measure flux rates before structural changes became overly pronounced. We measured an average rate of 0.019 μm/s (SD = 0.012) after DMSO addition to bipolar spindles and half-spindles, in 13 independent experiments (see Fig. 8D). This rate is not significantly different from the rate of flux in DMSO asters and suggests that the mechanisms of flux in the spindle, half-spindle, and DMSO-aster are likely to be identical and that the differences in rates observed

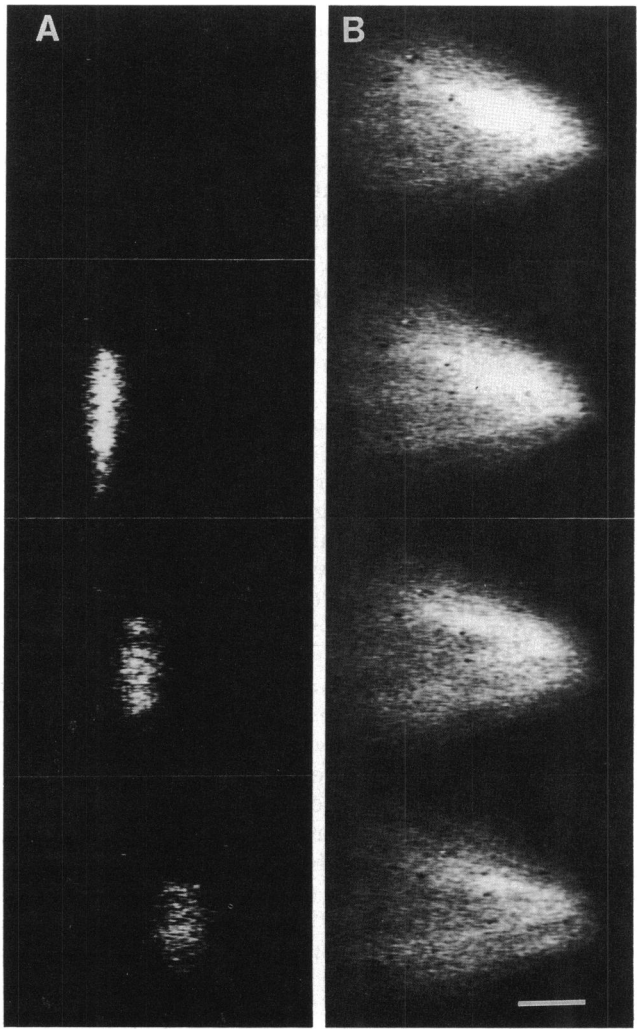

Figure 4. Poleward microtubule flux in an asymmetric DMSO-aster. Portions of video sequence showing (A) photoactivated caged-fluorescein tubulin and (B) total X-rhodamine tubulin fluorescence at 15 s before and 2, 172, and 342 s after photoactivation. Note both the rightward movement and decrease in intensity of the fluorescence peak. Scale bar, 10 μm.

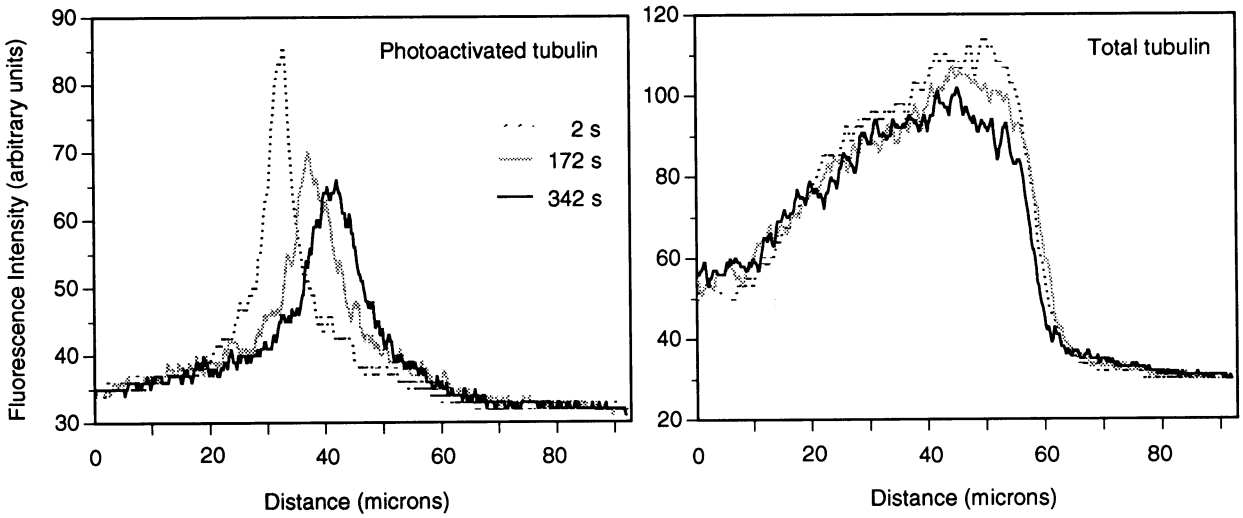

Figure 5. Fluorescence intensity profiles of the fluorescence images shown in Figure 4 at 2, 172, and 342 s after photoactivation.

in these different systems result from secondary effects of DMSO addition. The nature and number of targets of DMSO in this instance are unknown.

Role of the Eg5 Motor Protein in Poleward Flux

Eg5 is a kinesin-related motor protein involved in organizing the mitotic spindle and spindle poles (Le Guellec *et al.*, 1991; Sawin *et al.*, 1992). Because Eg5 is enriched toward spindle poles and a recombinant Eg5 fusion protein exhibits a slow (0.033 μm/s) plus-end directed microtubule motor activity in vitro, we have hypothesized that Eg5 might be directly involved in driving poleward microtubule flux (Sawin *et al.*, 1992). We tested this by photoactivating microtubule arrays in CSF extracts from which 96–98% of endogenous Eg5 had been removed by native immunoprecipitation. Under these conditions, in vitro spindle assembly is severely compromised and aberrant microtubule arrays are formed, although some apparently normal bipolar spindles are observed (Sawin *et al.*, 1992). Under the low-light conditions required for our experiments, we were unable to follow photoactivated marks and structural boundaries of aberrant microtubule arrays with great confidence. We therefore photoactivated fluorescence on the small fraction of bipolar spindles that did form ("Eg5-depleted spindles"). By immunofluorescence, these Eg5-depleted spindles showed a reduction in Eg5 staining to the same extent as that seen in aberrant arrays, confirming that Eg5-depleted spindles do not concentrate the small amount of Eg5 that remains in extracts after immunodepletion. As shown in Figure 6, photoactivated marks in Eg5-depleted spindles moved poleward at constant rates, with little change in spindle morphology over the course of experiments. Poleward movement of photoactivated fluorescence was also seen by digitization of fluorescence (Figure 7). The average rate of flux in Eg5-depleted extracts was 0.037 μm/s (SD = 0.014) (Figure 8E) and not significantly different from rates in half-spindle and "normal" bipolar spindles. The simplest interpretation of these results is that Eg5 is not directly involved in microtubule flux. These results are not completely definitive, however, as it is possible that the remaining 2–4% of endogenous Eg5 could be sufficient to drive poleward flux but nevertheless insufficient for proper spindle assembly. Although we consider this possibility unlikely, further extension of these results will require additional molecular tools to probe Eg5 function.

DISCUSSION

Poleward microtubule flux is merely one manifestation of a complex highly regulated behavior in which the steady-state structure of the mitotic spindle is maintained in a kind of dynamic balance, with coordinate tubulin polymerization at microtubule plus ends, depolymerization at minus ends, and movement of subunits of the microtubule lattice (Mitchison and Sawin, 1990). To begin to understand this dynamic behavior, we have examined the structural requirements for poleward flux, reducing the complexity of the spindle to more simplified spindle subassemblies. From these experiments we can conclude that neither antiparallel microtubules nor chromosomes are required for microtubule flux nor are conventional centrosomes. Because the centers of taxol- and DMSO-asters do accumulate some antigens that normally localize to the centrosome, we suspect that these astral centers contain at least some elements of what are typically considered to be part of the functional biochemistry of the centrosome; however, the relation of these astral centers to centrosomes and spindle poles remains unclear.

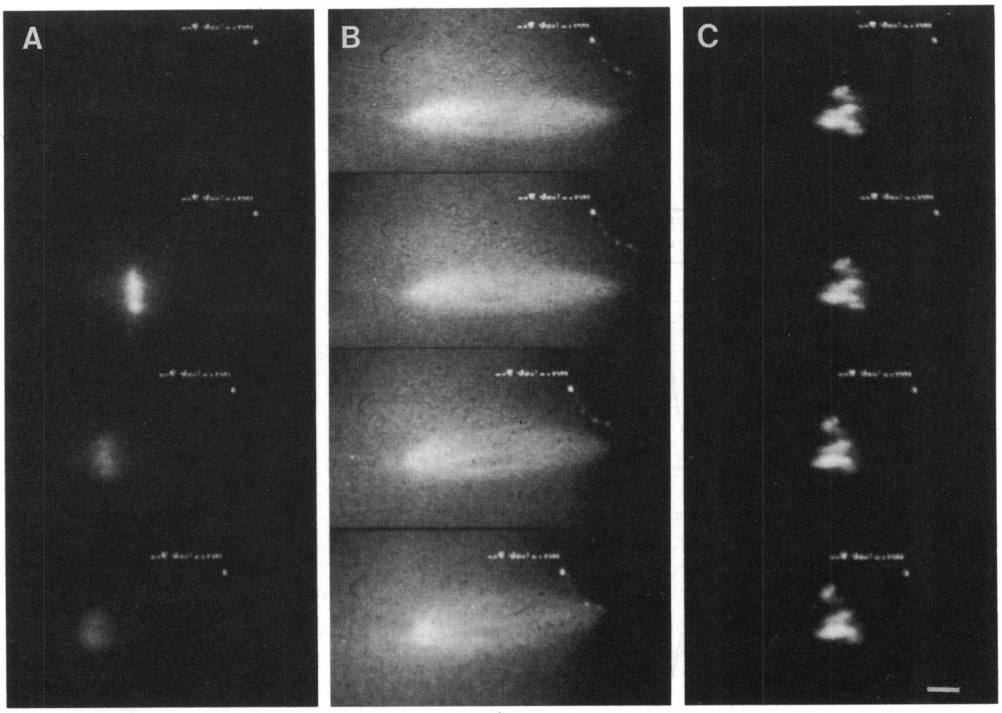

Figure 6. Microtubule flux persists in extracts immunodepleted of the Eg5 motor protein. Portions from a triple-label video sequence, showing (A) photoactivated caged-fluorescein tubulin, (B) X-rhodamine tubulin, and (C) CY5-labeled chromatin at 20 s before and 2, 156, and 308 s after photoactivation. Scale bar, 10 μm.

What are the elements of spindle architecture required for poleward microtubule flux and where does the force for flux originate? We note that at least two elements of microtubule organization are shared by both half-spindles and DMSO asters: dense microtubule bundles and some sort of morphological "pole," i.e., a constellation or local aggregate of microtubule minus ends. Our experiments suggest that the site of the motive force for flux is either at this pole or embedded in a matrix of material surrounding microtubule bundles. The results obtained with DMSO asters further indicate that if components of the flux machinery are indeed elements of the spindle pole, they do not require centrioles or a preexisting centrosome but rather are recruited readily from the cytoplasm to the site of force generation. This notion of "recruitment" to an incipient microtubule array is consistent with previous observations that individual or unbundled microtubules in CSF extracts are simply too unstable to exhibit any flux (see, for example, Belmont *et al.*, 1990). Correspondingly, in the few experiments where photoactivated marks were made on "early" half-spindles and DMSO asters (i.e., those that had not progressed very far along the morphogenetic pathway), these marks disappeared very rapidly, without any obvious poleward movement. By contrast, we did not observe "late" (i.e., well formed) structures that did not flux. Thus, partial stabilization of microtubule dynamics and poleward microtubule flux may correlate. What is not yet clear in this crude system is whether microtubule stabilization may precede the recruitment of the flux machinery or occur concomitantly with recruitment. This second possibility might obtain if, for example, motor proteins binding along the length of microtubules were to both drive poleward flux (see below) and stabilize dynamics. Further progress in this area depends on a firm molecular characterization of the flux motor.

Qualitatively, poleward flux resembles classical head-to-tail microtubule treadmilling, an in vitro behavior characteristic of microtubules with bound microtubule-associated proteins in which steady-state microtubule length is preserved, but microtubule plus-ends slowly polymerize and minus ends depolymerize (Hotani and Horio, 1988; Margolis and Wilson, 1978, 1981). The energy for this nonequilibrium steady-state process is derived from the hydrolysis of GTP accompanying tubulin polymerization. Because poleward flux is nearly two orders of magnitude faster than microtubule treadmilling in vitro, we have argued that the difference between rates of poleward flux and in vitro treadmilling is likely to reflect acceleration of intrinsic treadmilling by additional mechanisms (Sawin and Mitchison, 1991b), hence the search for a "motor." Based on our results, we can consider at least two mechanistic models to account for the force production required for poleward flux (Figure 9). Both of these views postulate a mechanism for increasing the lability of microtubule minus ends, which are typically quite stable both in vitro and in vivo (Inoue, 1964; Leslie and Pickett-Heaps, 1984; Tao *et al.*, 1987; Walker *et al.*, 1989; Wilson and Forer, 1988). Poleward flux requires that minus ends depolymerize at defined

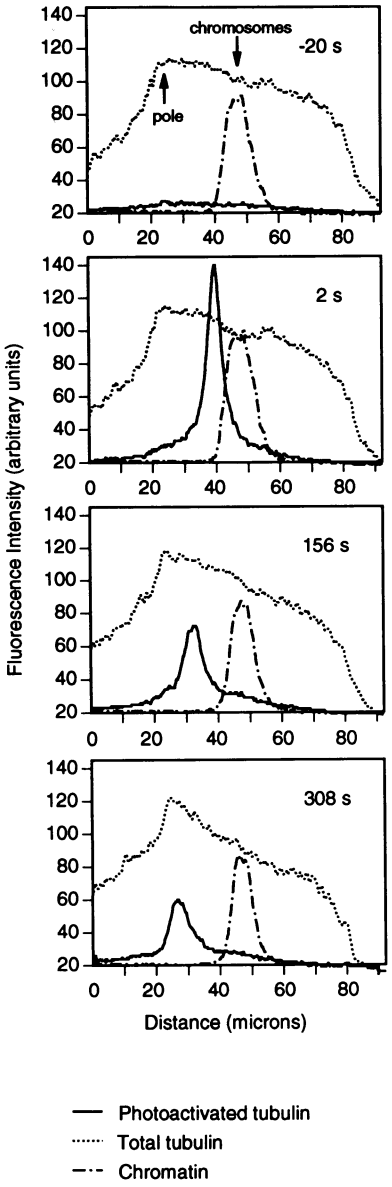

Figure 7. Fluorescence intensity profiles from the video sequence shown in Figure 6. The total tubulin fluorescence and the position of chromosomes remain essentially unchanged, whereas photoactivated fluorescence moves leftward and decreases in intensity.

rates, perhaps after being released from centrosomal nucleation sites (Sawin *et al.*, 1992). Indeed, one of the current challenges in understanding spindle architecture and dynamics lies in better understanding the biochemistry of spindle microtubule minus ends.

In the first model (Figure 9A), we envision acceleration of treadmilling by a pole- or matrix-bound microtubule motor protein, which would push (or pull, depending on its location) microtubule minus-ends into a depolymerization zone created by activities that, like centrosomal antigens, are predominantly at spindle poles. Minus-end depolymerization could be effected by local changes in the activity of factors that regulate microtubule dynamic instability or perhaps by microtubule severing proteins (Vale, 1991; Shiina *et al.*, 1992; McNally and Vale, 1993) localized to spindle poles. Our data suggest that Eg5 is unlikely to be a rate-limiting component of any motor-driven movement, whereas other likely candidate motors (which would most likely be plus-end directed) remain to be identified. It is also possible that the "depolymerase" and the motor could be members of the same supramolecular complex or perhaps even the same polypeptide, i.e., one that both "pulls" and "chews" at the same time. In this light it will be interesting to examine whether the recently purified microtubule-severing ATPase, katanin (McNally and Vale, 1993), might act processively in a manner that could generate force on a microtubule.

According to the second model (Figure 9B), the rate of minus-end depolymerization might itself be limiting

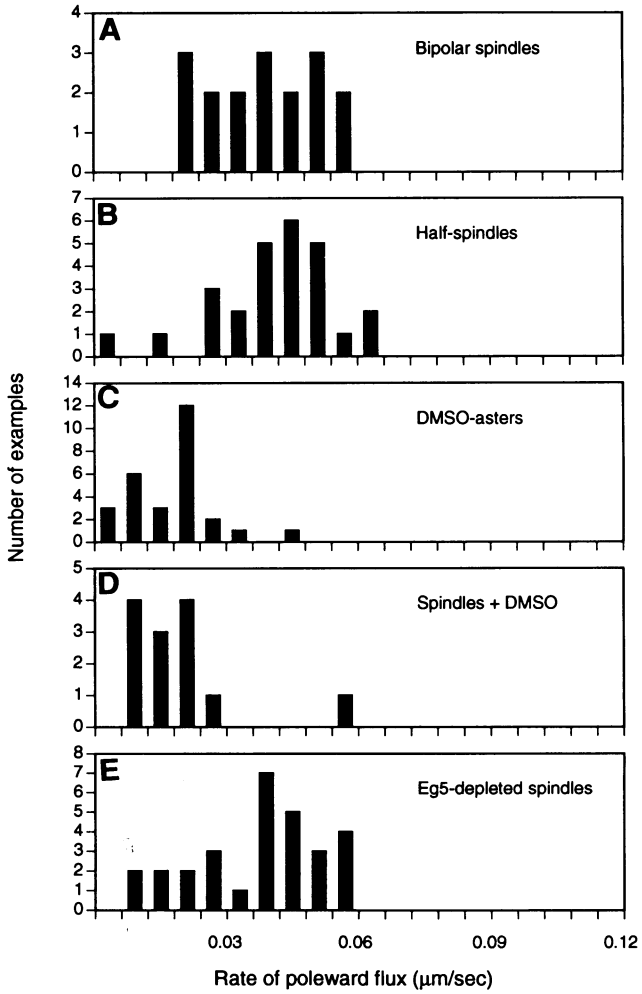

Figure 8. Rate histograms for poleward flux under the different conditions shown. See text for further details.

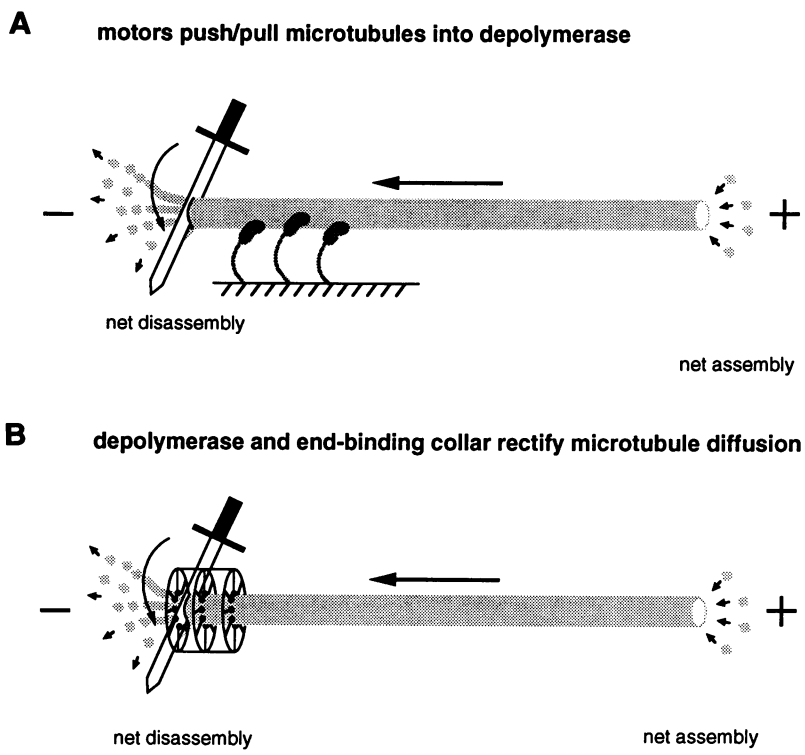

Figure 9. Two possible mechanisms for the force generation underlying poleward microtubule flux. Tubulin subunit addition is shown at microtubule plus ends and polymer disassembly at minus ends (spindle poles). The long arrow along the microtubule indicates the direction of flux movement. The minus-end depolymerizing activity is fancifully depicted as a sword, cutting the microtubule at or near the spindle pole. (A) Flux is driven by motor proteins (bean-shaped guys) that actively translocate a microtubule into the depolymerization zone. Although the motor is shown binding along the length of the microtubule, it also could be localized to the spindle pole or could be a part of the depolymerizing activity itself. (B) Flux is driven by thermal energy (one-dimensional microtubule diffusion) and rectified by depolymerization, acting in concert with a sliding collar of microtubule-binding proteins that localizes to the spindle pole. See text for further details.

and indirectly provide the motive force for flux via a mechanism of biased diffusion or a "thermal ratchet" (Koshland *et al.*, 1988; Simon *et al.*, 1992). In addition to a mechanism for depolymerizing minus ends, this second model posits a complex of proteins at the poles, bound to microtubules in the form of a sliding collar or sleeve. As tubulin subunits are progressively lost from minus ends, microtubule diffusion toward the spindle pole would be favored energetically over diffusion away from the pole, as unfilled microtubule-binding sites in the collar must be occupied to lower the total free energy of the system. We note that such a mechanism could include both equilibrium and kinetic components (Hill, 1985). According to this scheme, the motive force for poleward microtubule flux would be provided directly by thermal motion, whereas the vectorial nature of the movement would be derived energetically from the hydrolysis of nucleotide accompanying microtubule depolymerization. The thermal ratchet model may be confounded by the fact that a diffusing microtubule may also be in contact with a number of binding proteins that could retard diffusion or generate force in an opposing direction; nevertheless, the observation that antiparallel microtubules from opposing half-spindles can flux against each other while spindle structure is maintained suggests that the bonds that hold the spindle together are constantly being broken and remade, and thus the cell may have a means to circumvent these problems.

Models similar to both types presented here have been previously suggested for kinetochore function in vivo by many investigators (see, for example, Hill, 1985; Koshland *et al.*, 1988; Coue *et al.*, 1991; Gorbsky, 1992); it will be interesting to see how similar the two ends of spindle microtubules actually are.

ACKNOWLEDGMENTS

We are indebted to Paul Millman of Chroma Technologies (formerly of Omega Optical) for designing the interference filters used in these experiments and also to Terrell Hill for his analysis of kinetochore-microtubule interactions, from which some of our views on flux mechanism are derived. We thank Tim Stearns and Steve Salser for reading versions of the manuscript and UCSF Friends of Microtubules for helpful discussions, as well as John Sedat for use of his Cibachrome printer and Sue Parmelee for help with printing. We also thank the UCSF Markey Program in Biological Sciences for support of microscope facilities. This work was supported by grants from the NIH (GM39565) and from the Packard Foundation.

REFERENCES

Belmont, L.D., Hyman, A.A., Sawin, K.E., and Mitchison, T.J. (1990). Real-time visualization of cell cycle dependent changes in microtubule dynamics in cytoplasmic extracts. Cell *62*, 579–589.

Coue, M., Lombillo, V.A., and McIntosh, J.R. (1991). Microtubule depolymerization promotes particle and chromosome movement in vitro. J. Cell Biol. *112*, 1165–1175.

Gorbsky, G.J. (1992). Chromosome motion in mitosis. J. Cell Biol. *14*, 73–80.

Hill, T.L. (1985). Theoretical problems related to the attachment of microtubules to kinetochores. Proc. Natl. Acad. Sci. USA *82*, 4404–4408.

Hotani, H., and Horio, T. (1988). Dynamics of microtubules visualized by darkfield microscopy: treadmilling and dynamic instability. Cell Motil. Cytoskeleton *10*, 229–236.

Hyman, A., Drechsel, D., Kellogg, D., Salser, S., Sawin, K., Steffen, P., Wordeman, L., and Mitchison, T. (1991). Preparation of modified tubulins. Methods Enzymol. *196*, 478–485.

Inoue, S. (1964). Organization and function of the mitotic spindle. In: Primitive Motile Systems in Cell Biology, ed. R.D. Allen and N. Kamiya, New York: Academic Press, 549–598.

Inoue, S. (1981). Cell division and the mitotic spindle. J. Cell Biol. *91*, 131s–147s.

Inoue, S., and Ritter, H.J. (1975). Dynamics of mitotic spindle organization and function. In: Molecules and Cell Movement, ed., S. Inoue and R.E. Stephens, New York: Raven Press, 3–30.

Inoue, S., and Sato, H. (1967). Cell motility by labile association of molecules. The nature of mitotic spindle fibres and their role in chromosome movement. J. Gen. Physiol. *50*, 259–292.

Karsenti, E. (1991). Mitotic spindle morphogenesis in animal cells. Semin. Cell Biol. *2*, 251–260.

Koshland, D.E., Mitchison, T.J., and Kirschner, M.W. (1988). Polewards chromosome movement driven by microtubule depolymerization in vitro. Nature *331*, 499–504.

Le Guellec, R., Paris, J., Couturier, A., Roghi, C., and Philippe, M. (1991). Cloning by differential screening of a *Xenopus* cDNA that encodes a kinesin-related protein. Mol. Cell. Biol. *11*, 3395–3398.

Leslie, R.J., and Pickett-Heaps, J.D. (1984). Spindle microtubule dynamics following ultraviolet-microbeam irradiations of mitotic diatoms. Cell *36*, 717–727.

Margolis, R.L., and Wilson, L. (1978). Opposite end assembly and disassembly of microtubules at steady state in vitro. Cell *13*, 1–8.

Margolis, R.L., and Wilson, L. (1981). Microtubule treadmills—possible molecular machinery. Nature *293*, 705–711.

Mazia, D. (1961). Mitosis and the physiology of cell division. In: The Cell, vol. 3, ed. J. Brachet and A.E. Mirsky, New York: Academic Press, 77–412.

McIntosh, J.R., and Koonce, M.P. (1989). Mitosis. Science *246*, 622–628.

McNally, F.J., and Vale, R.D. (1993). Identification of katanin, an ATPase that severs and disassembles stable microtubules. Cell *75*, 419–429.

Mitchison, T.J. (1989). Polewards microtubule flux in the mitotic spindle: evidence from photoactivation of fluorescence. J. Cell Biol. *109*, 637–652.

Mitchison, T.J., and Kirschner, M.W. (1984). Dynamic instability of microtubule growth. Nature *312*, 237–242.

Mitchison, T.J., and Kirschner, M.W. (1985). Properties of the kinetochore in vitro. 2. Microtubule capture and ATP dependant translocation. J. Cell Biol. *101*, 767–777.

Mitchison, T.J., and Salmon, E.D. (1992). Kinetochore fiber movement contributes to anaphase-A in newt lung cells. J. Cell Biol. *119*, 569–582.

Mitchison, T.J., and Sawin, K.E. (1990). Tubulin flux in the mitotic spindle: where does it come from, where is it going? Cell Motil. Cytoskeleton *16*, 93–98.

Murray, A.W. (1992). Cell-cycle extracts. In: Methods in Cell Biology, ed. B.K. Kay and H.B. Peng, San Diego: Academic Press, 581–605.

Nicklas, R.B. (1971). Mitosis. Adv. Cell Biol. *2*, 225–297.

Rieder, C.L., Davison, E.A., Jensen, L.C.W., Cassimeris, L., and Salmon, E.D. (1986). Oscillatory movements of monooriented chromosomes and their position relative to the spindle pole result from the ejection properties of the aster and the half-spindle. J. Cell Biol. *103*, 581–591.

Salmon, E.D., Leslie, R.J., Karow, W.M., McIntosh, J.R., and Saxton, R.J. (1984). Spindle microtubule dynamics in sea urchin embryos. Analysis using fluorescence-labeled tubulin and measurements of fluorescence redistribution after laser photobleaching. J. Cell Biol. *99*, 2165–2174.

Sawin, K.E., LeGuellec, K., Philippe, M., and Mitchison, T.J. (1992). Mitotic spindle organization by a plus-end directed microtubule motor. Nature *359*, 540–543.

Sawin, K.E., and Mitchison, T.J. (1991a). Mitotic spindle assembly by two different pathways in vitro. J. Cell Biol. *112*, 925–940.

Sawin, K.E., and Mitchison, T.J. (1991b). Poleward microtubule flux in mitotic spindles assembled in vitro. J. Cell Biol. *112*, 941–954.

Sawin, K.E., Mitchison, T.J., and Wordeman, L.G. (1992). Evidence for kinesin-like proteins in the mitotic apparatus using peptide antibodies. J. Cell Sci. *102*, 303–313.

Sawin, K.E., Theriot, J.A., and Mitchison, T.J. (1993). Photoactivation of fluorescence as a probe for cytoskeletal dynamics in mitosis and cell motility. In: Fluorescent and Luminescent Probes for Biological Activity, ed. W.T. Mason, London: Academic Press, 405–419.

Saxton, W.M., Stemple, D.L., Leslie, R.J., Salmon, E.D., Zavortink, M., and McIntosh, J.R. (1984). Tubulin dynamics in cultured mammalian cells. J. Cell Biol. *99*, 2175–2186.

Shiina, N., Gotoh, Y., and Nishida, E. (1992). A novel homo-oligomeric protein responsible for an MPF-dependent microtubule-severing activity. EMBO J. *11*, 4723–4731.

Simon, S.M., Peskin, C.S., and Oster, G.F. (1992). What drives the translocation of proteins? Proc. Natl. Acad. Sci. USA *89*, 3770–3774.

Stearns, T., and Kirschner, M.W. (1994). In vitro reconstitution of centrosome assembly and function: the role of gamma tubulin. Cell (*in press*).

Tao, W., Walter, R.J., and Berns, M.W. (1987). Laser-transected microtubules exhibit individuality of regrowth, however most free new ends of the microtubules are stable. J. Cell Biol. *107*, 1025–1035.

Vale, R.D. (1991). Severing of stable microtubules by a mitotically activated protein in *Xenopus* egg extracts. Cell *64*, 827–839.

Verde, F., Berrez, J.-M., Antony, C., and Karsenti, E. (1991). Taxol-induced microtubule asters in mitotic extracts of *Xenopus* eggs: requirement for phosphorylated factors and cytoplasmic dynein. J. Cell Biol. *112*, 1177–1188.

Verde, F., Labbe, J.-C., Doree, M., and Karsenti, E. (1990). Regulation of microtubule dynamics by cdc2 protein kinase in cell-free extracts of *Xenopus* eggs. Nature *343*, 233–238.

Walker, R.A., Inoue, S., and Salmon, E.D. (1989). Asymmetric behavior of severed microtubule ends after ultraviolet-microbeam irradiation of individual microtubules in vitro. J. Cell Biol. *108*, 931–937.

Walker, R.A., O'Brien, E.T., Pryer, N.K., Sobeiro, M.F., Voter, W.A., Erickson, H.P., and Salmon, E.D. (1988). Dynamic instability of individual microtubules analysed by video light microscopy: rate constants and transition frequencies. J. Cell Biol. *107*, 1437.

Wilson, P.J., and Forer, A. (1988). Ultraviolet microbeam irradiation of chromosomal spindle fibers produces an area of reduced birefringence and shears the microtubules, allowing study of the dynamic behavior of new free ends in vivo. J. Cell Sci. *91*, 455–468.